Using a *P. falciparum* genetic cross to dissect the relative contributions of *pfcrt* and *plasmepsin II/III* to piperaquine response-related traits

John Kane[1], Xue Li[2], Sudhir Kumar[3], Katrina A. Button-Simons[1], Katelyn Vendrely Brenneman[4], Haley Dahlhoff[1], Mackenzie A.C. Sievert[1], Lisa A. Checkley[1], Douglas A. Shoue[1], Puspendra P. Singh[1], Meseret T. Haile[3], [2]Ann Reyes, Ian H. Cheeseman[5], Ashley M. Vaughan[3,6], Timothy J. C. Anderson[2], & Michael T. Ferdig[1]*.

[1]Eck Institute for Global Health, Department of Biological Sciences, University of Notre Dame, Notre Dame, IN, USA. [2]Disease Intervention and Prevention Program, Texas Biomedical Research Institute, San Antonio, TX, USA. [3]Center for Global Infectious Disease Research, Seattle Children's Research Institute, Seattle, WA, USA. [4]Harvard T.H. Chan School of Public Health, Boston, MA, USA. [5]Host Pathogen Interactions Program, Texas Biomedical Research Institute, San Antonio, TX, USA. [6]Department of Pediatrics, University of Washington, Seattle, WA, USA.

* Corresponding Author

Abstract

Piperaquine (PPQ) is widely used in combination with dihydroartemisinin (DHA) as a first-line treatment against malaria parasites. Resistance to this artemisinin combination therapy (ACT) has emerged in Cambodia and threatens to spread to other malaria-endemic regions. Multiple drivers of PPQ resistance have been reported, including mutations in the *Plasmodium falciparum chloroquine resistance transporter* (*pfcrt*) and increased copies of *plasmepsin II/III* (*pm*). Experimental genetic crosses allow for the precise quantification of the relative contributions of specific loci to a phenotype and have the distinct advantage of assaying the effects of naturally evolved genetic variation. We generated a cross between a Cambodia-derived multi-drug resistant KEL1/PLA1 lineage parasite isolate (KH004) and a drug susceptible parasite isolated in Malawi (Mal31). Mal31 harbors a wild-type (3D7-like*) pfcrt* allele and a single copy of *pm,* while KH004 has a chloroquine-resistant (Dd2-like*) pfcrt* allele with an additional G367C substitution and four copies of *pm*. We cloned 101 unique recombinant progeny from this cross, and from this pool, we identified a targeted set of progeny representing all possible combinations of variants *at pfcrt and pm* for detailed analysis of a range of PPQ response and competitive fitness phenotypes. Fortuitously, progeny clones that inherited the KH004 *pm* allele displayed a range of different

35 copies, allowing us to directly test the role *of pm* copy number on a range of resistance
36 phenotypes, including IC50, area under the curve (AUC), and PSA as well as competitive fitness.
37 We find that all progeny inheriting both *pfcrt* and *pm* alleles from KH004 are PPQ resistant by
38 (PSA and AUC) and that inheritance of KH004 *pfcrt* is required for resistance (including progeny
39 that inherited the single copy *pm* from Mal31). Our findings clearly display how progeny clones
40 from experimental crosses can be used to parse apart the contributions *of pfcrt, pm,* and parasite
41 genetic background*,* to a range of PPQ-related traits and confirm the critical role of the PfCRT
42 G367C substitution on PPQ resistance.
43
44 **Introduction**
45
46 Malaria is a life-threatening parasitic disease that nearly half of the world's population is
47 at risk of contracting (1). The World Health Organization estimates that in 2020 there were 247
48 million malaria cases and 619,000 deaths reported across 84 countries, with 76% of those deaths
49 occurring in children under the age of 5 (1). The continued evolution of drug-resistant *Plasmodium*
50 *falciparum* asexual blood-stage parasites has been one of the major obstacles to global malaria
51 elimination and eradication efforts (1). Current frontline treatments for uncomplicated *P.*
52 *falciparum* infection are artemisinin-based combination therapies (ACT), which are composed of
53 a fast-acting artemisinin (ART) derivative paired with one or more longer-lasting partner drugs (2).
54 ACTs began to replace historically efficient antimalarials, such as chloroquine (CQ) and
55 sulfadoxine-pyrimethamine (SP), as first-line therapies in the early 2000s after resistance to these
56 two therapies swept throughout Africa (3–5). The WHO has recommended ACTs for
57 uncomplicated malaria since 2006 due to their greater efficacy and decreased resistance
58 compared to other single-drug therapeutics, with the most common ACTs used in Southeast Asia
59 (SEA) being dihydroartemisinin/piperaquine (DHA+PPQ), artemether/lumefantrine (AL), and
60 artesunate/mefloquine (AS+MQ). The ACT combination DHA-PPQ has been most widely used

61 throughout the Greater Mekong Subregion (GMS) of SEA which has historically been a hotbed
62 for antimalarial drug resistance (6–8).
63
64 The spread of resistance to DHA+PPQ is largely attributed to the spread of the rapidly
65 expanding, multidrug-resistant KEL1/PLA1 lineage of parasites (9–11). This lineage of "superbug"
66 parasites emerged out of western Cambodia in 2008 and has since spread to Vietnam, Laos, and
67 northeastern Thailand in subsequent years (10). KEL1/PLA1 parasites are characterized by
68 mutations in *kelch13* (KEL1), specifically the C580Y substitution which has been strongly
69 associated with ART resistance, as well as a copy number (CN) amplification of the two aspartic
70 protease genes *plasmepsin II/III* (PLA1), which has been linked with decreased sensitivity to PPQ
71 (9, 10, 12, 13). The decreased sensitivity to ART derivatives results in a greater remaining parasite
72 load which has to be cleared by the partner drug, leading to an increased chance of ACT failure
73 (9, 14–17).
74
75 After the original detection of PPQ resistance in Cambodia in 2015, independent genome-
76 wide association studies identified that variation in *plasmepsin II/III* (*pm*) was associated with
77 PPQ-R parasites (16, 18–20). The proposed mechanism supporting the association between *pm*
78 amplification and PPQ-R is that plasmepsins reduce concentrations of reactive heme in the
79 parasite digestive vacuole (DV), which counters the inhibitory mechanism of PPQ (20). Increased
80 parasite survival at higher PPQ concentrations amongst Cambodian field isolates was shown to
81 be associated with amplification of *pm*, further connecting plasmepsins with a PPQ-R phenotype
82 (13). Further *in vitro* studies of *pm* amplification have found that in a PPQ-S 3D7 background,
83 inactivation of *pm* results in a mild increase in PPQ susceptibility, whereas overexpression of *pm*
84 alone did not impact parasite sensitivity to PPQ, artesunate (AS), or CQ (21, 22). While *pm* has
85 clearly been shown to impact parasite response to PPQ, variations of *in vitro* and isolate-based

genotype-phenotype associations suggest that while CN is associated with decreased sensitivity to PPQ, additional loci contribute to resistance (13, 23).

Additional to the role of *pm*, decreased copies of *pfmdr1* and single nucleotide polymorphisms (SNP) in several other genes, such as *exonuclease* (PF3D7_1362500) and the *Plasmodium falciparum chloroquine resistance transporter* (*pfcrt*) have been shown to contribute to PPQ-R (16, 18, 24–26). Novel haplotypes containing amino acid substitutions in PfCRT were originally identified due to their increasing prevalence in areas utilizing DHA+PPQ, and *in vitro* studies have found that edited isogenic parasites with these substitutions alone can impact parasite uptake of PPQ and drug sensitivity independent of *pm* copy number (25, 27–30). Field studies from within the GMS have noted that some of these *pfcrt* haplotypes have continued to expand within the last 5 years and are often found in parasites that also have multiple copies of *pm*, indicating no detrimental fitness cost associated with this allelic combination (31, 32). Additionally, the main PfCRT substitutions associated with PPQ-R, such as H97Y, F145I, M343L, G350R, and G353V, all arose from either a Dd2 or 7G8-like background (33, 34). This further connects genetic background to the original evolution of these resistance-conferring SNPs.

Compared to other antimalarials, assessing *in vitro* PPQ-R has been a challenge due to the shape of the dose-response curve in PPQ-R parasites. These resistant parasites show incomplete clearance at the higher concentrations used during phenotyping, resulting in a bimodal dose-response curve (13). To address this non-traditional curve shape, area under the curve (AUC) has been used as a proxy for traditional IC50 assays, with a greater AUC representing decreased sensitivity (13). Alternatively, the piperaquine survival assay (PSA) was developed to measure parasite survival rate after exposure to a pharmacologically relevant (200nM) dose of PPQ (18). While both measurements can correlate with overall PPQ-R, a multi-phenotype approach can not only validate the strongest factors driving resistance, which should be observed

112 in all phenotypes, but can potentially identify different secondary loci due to slight differences in
113 the measured phenotype.
114
115 To further understand the complexity and contributions of several loci to PPQ-R, we used
116 progeny from a genetic cross between a multidrug-resistant Cambodian parasite of KEL1/PLA1
117 lineage (KH004) and a drug-sensitive Malawi isolate (Mal31). KH004 carries a C508Y Kelch13, a
118 Dd2-like PfCRT (74I, 75E, 76T, 220S, 271E, 326S, 356T, and 371I) with an addition G367C
119 substitution, and 4 copies of *pm*. Mal31 has a wild-type genotype at both *kelch13* and *pfcrt* and
120 carries a single copy of *pm* (Figure 1A). The G367C substitution in PfCRT carried by KH004 has
121 previously been identified as a novel haplotype present in SEA, however, this is the first study
122 that directly connects it to *in vitro* PPQ resistance (25, 33, 35).
123
124 The genetic background of *P. falciparum* has continuously been shown to play a central
125 role in the emergence of drug resistance as well as supporting parasite fitness. While several
126 genetic factors have been implicated in PPQ resistance, understanding the epistatic interactions
127 between these loci is crucial for identifying parasites that can easily develop resistance or lineages
128 which have the potential to expand. A genetic cross-based approach to studying PPQ-R allows
129 for recombination across the entire genome and can identify the contributions of all loci, both
130 known and unidentified, when paired with linkage analysis such as quantitative trait loci (QTL)
131 mapping. In this study, we use three different phenotypes of resistance (limited-point IC50, AUS,
132 and PSA) to identify the contributions of a novel *pfcrt* haplotype and amplification of *pm* to PPQ
133 resistance as well as detect additional loci which further contribute to resistance and modulate
134 parasite fitness.
135
136
137

138 **Results**

139 ***Novel allelic combinations of pfcrt and plasmepsin II/III***

140 From our genetic cross between KH004 and Mal31, previously described in Brenneman
141 et al. (36), we recovered 101 unique recombinant progeny with various combinations of
142 inheritance of *pfcrt, plasmepsin II/III,* alleles and *pm* copy number, ranging from single copy to
143 five copies (Figure 1B). Genome-wide, we see two large skews in inheritance favoring Mal31
144 alleles on Chr 7 and 14 (Supplementary Figure 1A). Both of these skews towards the African
145 drug-sensitive parent have been observed in previous crosses, and indicate a potential fitness
146 cost associated with the inheritance of these alleles (37). Additionally, we see no evidence for
147 pairwise linkage disequilibrium or co-inheritance among these genes or other loci across the
148 genome, including when accounting for *pm* CN (Supplementary Figure 1B**)**.

149

150 ***PPQ dose response phenotype***

151 Traditional IC50 assays have not been useful in phenotyping PPQ resistance due to the
152 well-documented biphasic dose-response curve observed in PPQ-R parasites. Based on the
153 dose-response phenotypes of the progeny from our KH004 × Mal31 genetic cross, we find that
154 the combination of mutations in *pfcrt* plus multiple copies of *pm* is responsible for this biphasic
155 phenotype. Parasites with single copies of *pm*, as well as those which inherited the *pfcrt* allele
156 from Mal31, all display a traditional sigmoidal dose-response curve. Conversely, parasites that
157 carry the KH004 *pfcrt* allele while also expressing multiple copies of *pm* produce a biphasic curve.

158

159 ***PfCRT is the main driver of PPQ resistance***

160 One of the major challenges to phenotyping PPQ drug response is the biphasic dose-
161 response curve, indicating incomplete parasite killing at higher drug concentrations observed in
162 PPQ-R parasites. To study the response of parasites with novel combinations of *pfcrt* and *pm* to
163 PPQ independent of dose curve shape, the piperaquine survival assay (PSA) was performed on

164 48 progeny and both parents from the KH004 × Mal31 cross and encompassed all available
165 combinations of *pfcrt* and *pm* alleles and *pm* CN. Our results show a significant difference in PPQ
166 sensitivity based on the *pfcrt* genotype (Figure 2A). Within the PPQ-R population inheriting the
167 *pfcrt* allele from the KH004 parent, we further see an increase in resistance associated with an
168 increase in *pm* CN. Additionally, QTL mapping of the PSA phenotype revealed a highly significant
169 (1% threshold) 144 kb region on chromosome 7 (LOD score of 10.615), which encompasses *pfcrt*
170 (Figure 2B,). Additional measures of variance identify that this strong peak containing *pfcrt* is
171 responsible for 61.9**%** of the observed phenotypic variance in the PSA phenotype. Due to this
172 large and potentially masking effect of *pfcrt*, secondary scans of residual variation were used after
173 statistically removing the effect from the chromosome 7 locus. These residual scans identified
174 another highly significant (1% threshold, LOD score of 4.175) marker on chromosome 14 (Figure
175 2C). Using a 95% confidence interval (CI) from the highest LOD score, this secondary peak
176 contains the *plasmepsin II* gene. We further support the association between *pm* CN amplification
177 and PPQ resistance by using a secondary measure of resistance, AUC (Figure 2D-F). QTL
178 mapping based on the AUC phenotype identifies a strong peak on chromosome 7 (LOD 6.94),
179 similar to the one identified using PSA, which accounts for 48.4% of phenotypic variance (Figure
180 2E). Residual scans of this phenotype also identify a significant (5% threshold, LOD of 4.199)
181 marker on chromosome 10, which contains 61 genes (Supplementary Table 1).
182

183 ***Plasmepsin II/III plays an additive role in PPQ resistance***

184 Based on our data from PSA and AUC measurements, we identified that copy number
185 amplification of *pm* contributes to a decreased sensitivity to PPQ (Figure 2A, C, D). However, this
186 effect of copy number is often masked by *pfcrt* (Figure 2B). The main reason why IC50 is not
187 traditionally used for phenotyping PPQ is due to the biphasic drug response curve associated with
188 resistance. By using a limited point IC50 (LP-IC50), we can remove the biphasic portion of the

189 curve and therefore calculate an IC50 for PPQ. These results show an increased IC50 due to the
190 inheritance of the *pfcrt* allele as well as *pm* amplification in the Mal31 *pfcrt* population (Figure 3A).
191 However, this decreased sensitivity to PPQ reaches an IC50 of 6nm, which is still comparable to
192 other PPQ-S parasites such as 3D7 (21). Once again, QTL mapping of this phenotype identified
193 a strong association between IC50 and *pfcrt* (Figure 3B). While this IC50 phenotype was sufficient
194 to map the impact of *pfcrt*, it did not provide the same resolution in differentiating PPQ-R and
195 PPQ-S parasites as the other phenotypes did.
196
197 ***PfCRT G367C confers PPQ resistance***
198 Using progeny from our KH004×Mal31 genetic cross, we have further validated the results
199 of previous studies, which indicate that *pfcrt* is the main driver of PPQ resistance. From this
200 progeny set, inheritance of the *pfcrt* allele from KH004 was the major factor shared by PPQ-R
201 parasites (Figure 2,3). This parasite carries a Dd2-like *pfcrt* with the addition of a novel mutation
202 G367C. Most drug resistance-associated mutations in PfCRT are found in one of the 10
203 transmembrane (TM) domains, and specifically regions that make up the central cavity of the
204 transporter (33, 38). The G36C substitution differs from other PPQ-R-associated mutations in that
205 while it is found within TM9 with other known mutations, it is found in the digestive vacuole (DV)
206 exposed portion of this protein and does not part of the core structure of the transporter's central
207 cavity (Supplementary Figure 2). While the Dd2 *pfcrt* haplotype confers to resistance to other
208 antimalarials, such as CQ, the haplotype does not confer PPQ resistance, indicating the direct
209 influence of the G367C mutation. To validate this, we used PSA to measure PPQ sensitivity
210 between Dd2, KH004, a selfed KH004 parasite from our cross, which carries only a single copy
211 of *plasmepsin II/II, and* NHP4026 which is from SEA and also expresses a Dd2 *pfcrt*. PSA reveals
212 that both parasites containing the G367C SNP are significantly less sensitive to PPQ compared
213 to the Dd2 parasite, which lacks that mutation (Supplementary Figure 3).
214

215 This novel G367C mutation has previously been mentioned by Ross et al (25) for its
216 presence in SEA but was not globally prevalent at the time of analysis. Since the KEL1/PLA1
217 lineage has continued to spread throughout SEA and PPQ resistance has continued to emerge,
218 we analyzed the current prevalence of this novel mutation using the MalariaGen Pf7 dataset. Out
219 of 16,203 global *pfcrt* haplotypes, 29 samples carried the G367C substitution (Figure 4). This
220 substitution was originally identified in 2012 and was restricted to Cambodia but has emerged in
221 neighboring countries Vietnam and Laos since 2017 (Supplementary Table 2). Additionally, 93%
222 (27/29) of these filed samples also carry multiple copies of *pm*.
223
224 To further identify selective pressures on *pfcrt* in Cambodia, Laos, and Vietnam, we used
225 Tajima's D and nucleotide diversity to characterize positive selective pressure on this gene
226 (Figure 4). A Tajima's D value <2 results from a significant abundance in rare alleles that deviates
227 from expected mutation-drift equilibrium, indicative of positive selection on the gene. While *pfcrt*
228 remains in equilibrium with no selective pressures in Cambodia and Vietnam, we observed
229 significant positive selection for this gene in Laos (D= -2.718 p = 0.007) (Figure 4). Measurements
230 of Tajima's D over time also indicate that this positive selection event is recent, with a significant
231 negative Tajima's D score being observed only in 2018 (Supplementary Figure 4).
232
233 ***Impacts of pfcrt and pm inheritance on parasite fitness***
234 Our data across multiple resistance phenotypes support that *pfcrt* is the primary driver of PPQ-
235 R, with an additive increase in resistance resulting from increased copies of *pm.* It has also been
236 well-documented that mutations in major resistance-associated genes can be associated with a
237 loss in parasite fitness (30, 39, 40). For these novel resistance-conferring genotypes to increase
238 in global prevalence, parasites need to preserve fitness either through low-cost resistance
239 mutations or the acquisition of secondary compensatory mutations that preserve or improve
240 fitness. As a measurement of blood-stage fitness, we performed competitive growth assays

241 between progeny of the KH004 × Mal31 cross and both parental parasites (Supplementary Figure
242 5). These co-cultures were maintained for a maximum of 40 days or until one parasite reached
243 fixation (>90% of culture), with samples being collected every 7 days. Progeny vs. parent
244 competitions revealed that the majority of progeny had a fitness level between the two parents,
245 and four parasites were outside of the fitness range of the parents (two more fit than KH004 and
246 two less fit than Mal31), with no significant clustering in fitness based on inherited *pfcrt* and *pm*
247 genotypes (Supplementary Figure 5).
248
249 Based on the similar fitness phenotypes generated from competitions against the parental
250 parasites, a select subset of 18 progeny and both parents were set up in overlapping competitions
251 against common competitors, resulting in 212 competitive outcomes (win, lose, or draw). The
252 outcomes of these pairwise competitions were used to generate an Elo Rating for each parasite
253 using the *EloRating* package in R (41). This Elo phenotype has previously been used in ranking
254 dominance rankings but has not been adapted for ranking *P. falciparum* fitness hierarchies. Elo
255 ratings provide a weighted ranking of parasite fitness based on competitive growth outcome as
256 well as the fitness ranking of the competitor, with a higher Elo Rating representing a greater
257 competitive fitness level. Elo Ratings for these 20 parasites provide a much finer resolution of
258 fitness differences between parasites of seemingly similar fitness. Similar to competitions against
259 both parents, Elo Rating does not cluster based on *pfcrt* and *plasmepsin* genotype (Figure 5A).
260 However, QTL analysis using Elo phenotypes reveals a highly significant (1% threshold) on
261 chromosome 9 (LOD score of 4.489), which encompasses a 35kb region containing 15 genes
262 (Figure 5B). Parasites with the greatest competitive fitness were associated with inheritance of
263 this 35kb region from the KH004 parent Sequence comparison between KH004 and Mal31 for
264 these 15 genes identified 4 coding SNPs in two genes: PF3D7_0934100 and PF3D7_0934700
265 (Supplementary Table 3). In order to isolate the role of *pm* CN variation with respect to parasite
266 fitness, we compared fitness levels of two sets of isogenic progeny as well as parental parasites,

267 which have been selfed and varied in copy number in our competitive growth assays and
268 generated Elo ratings (Supplementary Figure 6). Based on these Elo scores, we observe no major
269 influence of *pm* CN alone on parasite fitness.
270
271
272 **Discussion**
273 In this study, we used a genetic cross between a multidrug-resistant Cambodian parasite
274 and a drug-sensitive isolate from Malawi to characterize the genetic contributors to PPQ-R.
275 Previous work on this subject has either utilized naturally resistant patient isolates or conducted
276 *in vitro* manipulations to confer PPQ-R (13, 16, 20, 25). By using a genetic cross, we can track
277 the inheritance of alleles that have previously been associated with resistance, such as SNPs in
278 PfCRT or amplification of *pm*, while accounting for variation in the parasite's genetic background.
279 Within our progeny set, we have identified that the inheritance of the KH004 PfCRT (Dd2 +
280 G367C) is the main driver of PPQ-R, with the amplification of *pm* serving an additive role amongst
281 resistant parasites.
282
283 The KH004 parent of this cross expresses a novel G367C substitution in PfCRT, which
284 has previously been identified in SEA but has never been associated with *in vitro* resistance to
285 PPQ. Through comparisons between KH004, Dd2, and other Southeast Asian parasites, we
286 observed a > 30-fold change in PSA between KH004 and parasites not expressing a Dd2-like
287 PfCRT, indicating a direct connection between this substitution and PPQ-R. While the G367C
288 substitution has not previously been connected to PPQ-R, this residue is within the binding site
289 of the structurally similar chloroquine derivative perfluorophenylazido biotinylated chloroquine
290 (AzBCQ) (42). Through the association of this residue with PPQ-R, we have contributed to a
291 further understanding of structural regions of PfCRT that influence resistance to PPQ. While we
292 have shown that the addition of the G367C substitution confers PPQ-R, the overall *pfcrt* haplotype

293 is likely what facilitates the evolution of these resistance-conferring SNPs. The major *pfcrt*
294 haplotypes associated with PPQ-R have all come out of a 7G8 or Dd2 background, and
295 transfection of these mutations into different *pfcrt* backgrounds has led to slight decreases in
296 resistance compared to those in a Dd2 background (28, 33).
297
298 Previously studied PPQ-R-associated PfCRT substitutions such as T93S, H97Y, C101F,
299 F145I, M343L, and G353V were originally identified based on their growing prevalence in areas
300 using the ACT DHA+PPQ (25, 33). The novel G367C substitution expressed by KH004 arose in
301 western Cambodia in 2012 and was found at a low abundance in the population, which is why it
302 had been overlooked compared to other mutations. Since its initial emergence, the Dd2+G367C
303 haplotype has continued to persist at a consistently low abundance but has spread to neighboring
304 countries, Laos and Vietnam, with the latter accounting for the majority of identifications in recent
305 years. As most of SEA has transitioned from DHA+PPQ to AL as the frontline ACT, Vietnam
306 continues to use PPQ, which might explain the recent increase in abundance of this novel
307 haplotype within the country (1). On the other hand, the introduction of this haplotype into Laos
308 can potentially be accounted for by a recent introduction of PPQ-R parasites into the country from
309 Cambodia (43).
310
311 Due to the difficult nature of phenotyping PPQ-R, we used 3 previously utilized resistance
312 phenotypes: AUC, limited point IC50, and PSA. By using these different assays, we can break
313 the resistance phenotype into three components, survival under high single dose PPQ (PSA), low
314 dose growth inhibition (IC50), and shape of the dose-response curve under high PPQ
315 concentrations (AUC), to identify the genetic factors driving variation within each of these
316 phenotypes (13, 18, 21, 22). All three of these phenotypes were able to identify PfCRT as the
317 main underlying contributor to resistance but identified different secondary loci for each
318 phenotype. QTL scans based on PSA phenotype after removing the large effect of *pfcrt* further

319 identify a region on chromosome 14 containing *plasmepsin II* as a secondary contributor to
320 resistance. This association supports the additive effect of *pm* copy number amplification
321 observed in our PPQ-R progeny (Figure 2). Using the AUC phenotype supported the strong
322 impact of *pfcrt*, but also identified a secondary association between the phenotype and a locus
323 on chromosome 10. One of the genes with the strongest association within this region is
324 *autophagy-related gene 18* (*atg18*). This protein, which localizes to the parasite DV, has
325 previously been associated with decreased sensitivity to several antimalarials such as DHA,
326 artemether (AM), and PPQ, while also being connected to increased survival under nutrient
327 deprivation (44–46). Due to its previous association with PPQ-R and the association only with the
328 AUC phenotype, *atg18* may potentially be one of the underlying factors for the non-traditional
329 dose-response curve encountered when studying *in vitro* PPQ-R
330
331 Previous studies into the impact of *pm* amplification have hypothesized that instead of
332 directly modulating PPQ-R, expressing multiple copies of this gene might serve a compensatory
333 role in parasite fitness (22). This hypothesis, paired with extensive previous findings on the fitness
334 costs of *pfcrt* resistance mutations, led us to assess the competitive fitness levels of our progeny
335 with various combinations of *pfcrt* and *pm* (29, 39, 47). We found that compared to the KH004
336 and Mal31 parents of this cross, there was no significant clustering of *pfcrt/pm* genotype
337 combinations that were associated with parasite fitness. Additionally, we have utilized Elo ratings
338 as a new way to assess parasite fitness within our set of progeny. Elo ratings are an effective
339 method for efficiently comparing head-to-head fitness levels across a large progeny set and
340 provide a more refined phenotype, which is necessary for effective QTL mapping. Using this Elo
341 phenotype, we have been able to identify a highly significant association between parasite fitness
342 and a narrow 35kb region on chromosome 9. This region is mainly composed of genes involved
343 in development, transcriptional regulation, and metabolism and contains two genes with coding
344 region SNP differences between KH004 and Mal31. Neither of these genes have previously been

345 directly connected to parasite fitness and therefore require future work to further examine the role
346 that they play in parasite fitness.
347
348 Understanding the genetic determinants of PPQ resistance is essential for future control
349 and prevention measures. Through our genetic cross, we have confirmed the major drivers of
350 resistance, including a novel *pfcrt* mutation, as well as identified secondary genetic factors that
351 contribute to parasite resistance and fitness. Additionally, we have been able to incorporate
352 several previously used PPQ-R phenotypes into our analysis and identify unique genetic regions
353 that are associated with changes in each phenotype. By combining this novel genetic cross with
354 rigorous *in vitro* resistance and fitness phenotyping, we have identified the genetic architecture
355 which promotes decreased sensitivity to PPQ while remaining competitively fit. While the
356 DHA+PPQ ACT continues to be used as a frontline ACT, it is crucial to understand the genetic
357 underpinnings of resistance. Furthermore, this genetic cross also highlights the recombination
358 events that would be required to confer PPQ-R if one of these multidrug resistant parasite lineages
359 were to expand to Africa.
360

References

1. World Health Organization. 2022. World malaria report 2022. Geneva.
2. White NJ, Pukrittayakamee S, Hien TT, Faiz MA, Mokuolu OA, Dondorp AM. 2014. Malaria. The Lancet 383:723–735.
3. Blasco B, Leroy D, Fidock DA. 2017. Antimalarial drug resistance: linking Plasmodium falciparum parasite biology to the clinic. Nat Med 23:917–928.
4. Payne D. 1987. Spread of chloroquine resistance in Plasmodium falciparum. Parasitol Today 3:241–246.
5. Mita T, Tanabe K, Kita K. 2009. Spread and evolution of Plasmodium falciparum drug resistance. Parasitol Int 58:201–209.
6. Imwong M, Suwannasin K, Kunasol C, Sutawong K, Mayxay M, Rekol H, Smithuis FM, Hlaing TM, Tun KM, van der Pluijm RW, Tripura R, Miotto O, Menard D, Dhorda M, Day NPJ, White NJ, Dondorp AM. 2017. The spread of artemisinin-resistant Plasmodium falciparum in the Greater Mekong subregion: a molecular epidemiology observational study. Lancet Infect Dis 17:491–497.
7. Imwong M, Dhorda M, Myo Tun K, Thu AM, Phyo AP, Proux S, Suwannasin K, Kunasol C, Srisutham S, Duanguppama J, Vongpromek R, Promnarate C, Saejeng A, Khantikul N, Sugaram R, Thanapongpichat S, Sawangjaroen N, Sutawong K, Han KT, Htut Y, Linn K, Win AA, Hlaing TM, van der Pluijm RW, Mayxay M, Pongvongsa T, Phommasone K, Tripura R, Peto TJ, von Seidlein L, Nguon C, Lek D, Chan XHS, Rekol H, Leang R, Huch C, Kwiatkowski DP, Miotto O, Ashley EA, Kyaw MP, Pukrittayakamee S, Day NPJ, Dondorp AM, Smithuis FM, Nosten FH, White NJ. 2020. Molecular epidemiology of resistance to antimalarial drugs in the Greater Mekong subregion: an observational study. Lancet Infect Dis 20:1470–1480.
8. Ecker A, Lehane AM, Clain J, Fidock DA. 2012. PfCRT and its role in antimalarial drug resistance. Trends in Parasitology 28:504–514.
9. Amato R, Pearson RD, Almagro-Garcia J, Amaratunga C, Lim P, Suon S, Sreng S, Drury E, Stalker J, Miotto O, Fairhurst RM, Kwiatkowski DP. 2018. Origins of the current outbreak of multidrug-resistant malaria in southeast Asia: a retrospective genetic study. Lancet Infect Dis 18:337–345.
10. Hamilton WL, Amato R, van der Pluijm RW, Jacob CG, Quang HH, Thuy-Nhien NT, Hien TT, Hongvanthong B, Chindavongsa K, Mayxay M, Huy R, Leang R, Huch C, Dysoley L, Amaratunga C, Suon S, Fairhurst RM, Tripura R, Peto TJ, Sovann Y, Jittamala P, Hanboonkunupakarn B, Pukrittayakamee S, Chau NH, Imwong M, Dhorda M, Vongpromek R, Chan XHS, Maude RJ, Pearson RD, Nguyen T, Rockett K, Drury E, Gonçalves S, White NJ, Day NP, Kwiatkowski DP, Dondorp AM, Miotto O. 2019. Evolution and expansion of multidrug-resistant malaria in southeast Asia: a genomic epidemiology study. Lancet Infect Dis 19:943–951.
11. MalariaGEN Plasmodium falciparum Community Project. 2016. Genomic epidemiology of artemisinin resistant malaria. Elife 5:e08714.
12. MalariaGEN, Abdel Hamid MM, Abdelraheem MH, Acheampong DO, Ahouidi A, Ali M, Almagro-Garcia J, Amambua-Ngwa A, Amaratunga C, Amenga-Etego L, Andagalu B, Anderson T, Andrianaranjaka V, Aniebo I, Aninagyei E, Ansah F, Ansah PO, Apinjoh T, Arnaldo P, Ashley E, Auburn S, Awandare GA, Ba H, Baraka V, Barry A, Bejon P, Bertin GI, Boni MF, Borrmann S, Bousema T, Bouyou-Akotet M, Branch O, Bull PC, Cheah H, Chindavongsa K, Chookajorn T, Chotivanich K, Claessens A, Conway DJ, Corredor V, Courtier E, Craig A, D'Alessandro U, Dama S, Day N, Denis B, Dhorda M, Diakite M, Djimde A, Dolecek C, Dondorp A, Doumbia S, Drakeley C, Drury E, Duffy P, Echeverry DF, Egwang TG, Enosse SMM, Erko B, Fairhurst RM, Faiz A, Fanello CA, Fleharty M, Forbes M, Fukuda M, Gamboa D, Ghansah A, Golassa L, Goncalves S, Harrison GLA, Healy SA, Hendry JA, Hernandez-Koutoucheva A, Hien TT, Hill CA, Hombhanje F, Hott A, Htut Y, Hussein M, Imwong M, Ishengoma D, Jackson SA, Jacob CG, Jeans J, Johnson KJ, Kamaliddin C, Kamau E, Keatley J, Kochakarn T, Konate DS, Konaté A, Kone A, Kwiatkowski DP, Kyaw MP, Kyle D, Lawniczak M, Lee SK, Lemnge M, Lim P, Lon C, Loua KM, Mandara CI, Marfurt J, Marsh K, Maude RJ, Mayxay M, Maïga-Ascofaré O, Miotto O, Mita T, Mobegi V,

412 Mohamed AO, Mokuolu OA, Montgomery J, Morang'a CM, Mueller I, Murie K, Newton PN, Ngo
413 Duc T, Nguyen T, Nguyen T-N, Nguyen Thi Kim T, Nguyen Van H, Noedl H, Nosten F, Noviyanti
414 R, Ntui VN-N, Nzila A, Ochola-Oyier LI, Ocholla H, Oduro A, Omedo I, Onyamboko MA,
415 Ouedraogo J-B, Oyebola K, Oyibo WA, Pearson R, Peshu N, Phyo AP, Plowe CV, Price RN,
416 Pukrittayakamee S, Quang HH, Randrianarivelojosia M, Rayner JC, Ringwald P, Rosanas-Urgell A,
417 Rovira-Vallbona E, Ruano-Rubio V, Ruiz L, Saunders D, Shayo A, Siba P, Simpson VJ, Sissoko
418 MS, Smith C, Su X, Sutherland C, Takala-Harrison S, Talman A, Tavul L, Thanh NV, Thathy V,
419 Thu AM, Toure M, Tshefu A, Verra F, Vinetz J, Wellems TE, Wendler J, White NJ, Whitton G,
420 Yavo W, Van Der Pluijm RW. 2023. Pf7: an open dataset of Plasmodium falciparum genome
421 variation in 20,000 worldwide samples. Wellcome Open Res 8:22.
422 13. Bopp S, Magistrado P, Wong W, Schaffner SF, Mukherjee A, Lim P, Dhorda M, Amaratunga C,
423 Woodrow CJ, Ashley EA, White NJ, Dondorp AM, Fairhurst RM, Ariey F, Menard D, Wirth DF,
424 Volkman SK. 2018. Plasmepsin II–III copy number accounts for bimodal piperaquine resistance
425 among Cambodian Plasmodium falciparum. Nat Commun 9:1769.
426 14. Anderson TJC, Nair S, McDew-White M, Cheeseman IH, Nkhoma S, Bilgic F, McGready R,
427 Ashley E, Pyae Phyo A, White NJ, Nosten F. 2017. Population Parameters Underlying an Ongoing
428 Soft Sweep in Southeast Asian Malaria Parasites. Mol Biol Evol 34:131–144.
429 15. Ariey F, Witkowski B, Amaratunga C, Beghain J, Langlois A-C, Khim N, Kim S, Duru V, Bouchier
430 C, Ma L, Lim P, Leang R, Duong S, Sreng S, Suon S, Chuor CM, Bout DM, Ménard S, Rogers
431 WO, Genton B, Fandeur T, Miotto O, Ringwald P, Le Bras J, Berry A, Barale J-C, Fairhurst RM,
432 Benoit-Vical F, Mercereau-Puijalon O, Ménard D. 2014. A molecular marker of artemisinin-
433 resistant Plasmodium falciparum malaria. Nature 505:50–55.
434 16. Amato R, Lim P, Miotto O, Amaratunga C, Dek D, Pearson RD, Almagro-Garcia J, Neal AT, Sreng
435 S, Suon S, Drury E, Jyothi D, Stalker J, Kwiatkowski DP, Fairhurst RM. 2017. Genetic markers
436 associated with dihydroartemisinin–piperaquine failure in Plasmodium falciparum malaria in
437 Cambodia: a genotype–phenotype association study. The Lancet Infectious Diseases 17:164–173.
438 17. Tumwebaze PK, Conrad MD, Okitwi M, Orena S, Byaruhanga O, Katairo T, Legac J, Garg S,
439 Giesbrecht D, Smith SR, Ceja FG, Nsobya SL, Bailey JA, Cooper RA, Rosenthal PJ. 2022.
440 Decreased susceptibility of Plasmodium falciparum to both dihydroartemisinin and lumefantrine in
441 northern Uganda. Nat Commun 13:6353.
442 18. Duru V, Khim N, Leang R, Kim S, Domergue A, Kloeung N, Ke S, Chy S, Eam R, Khean C, Loch
443 K, Ken M, Lek D, Beghain J, Ariey F, Guerin PJ, Huy R, Mercereau-Puijalon O, Witkowski B,
444 Menard D. 2015. Plasmodium falciparum dihydroartemisinin-piperaquine failures in Cambodia are
445 associated with mutant K13 parasites presenting high survival rates in novel piperaquine in vitro
446 assays: retrospective and prospective investigations. BMC Med 13:305.
447 19. Amaratunga C, Lim P, Suon S, Sreng S, Mao S, Sopha C, Sam B, Dek D, Try V, Amato R,
448 Blessborn D, Song L, Tullo GS, Fay MP, Anderson JM, Tarning J, Fairhurst RM. 2016.
449 Dihydroartemisinin-piperaquine resistance in Plasmodium falciparum malaria in Cambodia: a
450 multisite prospective cohort study. Lancet Infect Dis 16:357–365.
451 20. Witkowski B, Duru V, Khim N, Ross LS, Saintpierre B, Beghain J, Chy S, Kim S, Ke S, Kloeung
452 N, Eam R, Khean C, Ken M, Loch K, Bouillon A, Domergue A, Ma L, Bouchier C, Leang R, Huy
453 R, Nuel G, Barale J-C, Legrand E, Ringwald P, Fidock DA, Mercereau-Puijalon O, Ariey F,
454 Ménard D. 2017. A surrogate marker of piperaquine-resistant Plasmodium falciparum malaria: a
455 phenotype–genotype association study. The Lancet Infectious Diseases 17:174–183.
456 21. Mukherjee A, Gagnon D, Wirth DF, Richard D. 2018. Inactivation of Plasmepsins 2 and 3
457 Sensitizes Plasmodium falciparum to the Antimalarial Drug Piperaquine. Antimicrob Agents
458 Chemother 62.
459 22. Loesbanluechai D, Kotanan N, de Cozar C, Kochakarn T, Ansbro MR, Chotivanich K, White NJ,
460 Wilairat P, Lee MCS, Gamo FJ, Sanz LM, Chookajorn T, Kümpornsin K. 2019. Overexpression of
461 plasmepsin II and plasmepsin III does not directly cause reduction in Plasmodium falciparum
462 sensitivity to artesunate, chloroquine and piperaquine. Int J Parasitol Drugs Drug Resist 9:16–22.

463 23. Parobek CM, Parr JB, Brazeau NF, Lon C, Chaorattanakawee S, Gosi P, Barnett EJ, Norris LD,
464 Meshnick SR, Spring MD, Lanteri CA, Bailey JA, Saunders DL, Lin JT, Juliano JJ. 2017. Partner-
465 Drug Resistance and Population Substructuring of Artemisinin-Resistant Plasmodium falciparum in
466 Cambodia. Genome Biol Evol 9:1673–1686.
467 24. Boonyalai N, Vesely BA, Thamnurak C, Praditpol C, Fagnark W, Kirativanich K, Saingam P,
468 Chaisatit C, Lertsethtakarn P, Gosi P, Kuntawunginn W, Vanachayangkul P, Spring MD, Fukuda
469 MM, Lon C, Smith PL, Waters NC, Saunders DL, Wojnarski M. 2020. Piperaquine resistant
470 Cambodian Plasmodium falciparum clinical isolates: in vitro genotypic and phenotypic
471 characterization. Malar J 19:269.
472 25. Ross LS, Dhingra SK, Mok S, Yeo T, Wicht KJ, Kümpornsin K, Takala-Harrison S, Witkowski B,
473 Fairhurst RM, Ariey F, Menard D, Fidock DA. 2018. Emerging Southeast Asian PfCRT mutations
474 confer Plasmodium falciparum resistance to the first-line antimalarial piperaquine. Nat Commun
475 9:3314.
476 26. Dondorp AM. 2017. New genetic marker for piperaquine resistance in Plasmodium falciparum. The
477 Lancet Infectious Diseases 17:119–121.
478 27. Okombo J, Mok S, Qahash T, Yeo T, Bath J, Orchard LM, Owens E, Koo I, Albert I, Llinás M,
479 Fidock DA. 2022. Piperaquine-resistant PfCRT mutations differentially impact drug transport,
480 hemoglobin catabolism and parasite physiology in Plasmodium falciparum asexual blood stages.
481 PLoS Pathog 18:e1010926.
482 28. Wicht KJ, Small-Saunders JL, Hagenah LM, Mok S, Fidock DA. 2022. Mutant PfCRT Can Mediate
483 Piperaquine Resistance in African Plasmodium falciparum With Reduced Fitness and Increased
484 Susceptibility to Other Antimalarials. J Infect Dis 226:2021–2029.
485 29. Small-Saunders JL, Hagenah LM, Wicht KJ, Dhingra SK, Deni I, Kim J, Vendome J, Gil-Iturbe E,
486 Roepe PD, Mehta M, Mancia F, Quick M, Eppstein MJ, Fidock DA. 2022. Evidence for the early
487 emergence of piperaquine-resistant Plasmodium falciparum malaria and modeling strategies to
488 mitigate resistance. PLoS Pathog 18:e1010278.
489 30. Dhingra SK, Gabryszewski SJ, Small-Saunders JL, Yeo T, Henrich PP, Mok S, Fidock DA. 2019.
490 Global Spread of Mutant PfCRT and Its Pleiotropic Impact on Plasmodium falciparum Multidrug
491 Resistance and Fitness. mBio 10:e02731-18.
492 31. van der Pluijm RW, Imwong M, Chau NH, Hoa NT, Thuy-Nhien NT, Thanh NV, Jittamala P,
493 Hanboonkunupakarn B, Chutasmit K, Saelow C, Runjarern R, Kaewmok W, Tripura R, Peto TJ,
494 Yok S, Suon S, Sreng S, Mao S, Oun S, Yen S, Amaratunga C, Lek D, Huy R, Dhorda M,
495 Chotivanich K, Ashley EA, Mukaka M, Waithira N, Cheah PY, Maude RJ, Amato R, Pearson RD,
496 Gonçalves S, Jacob CG, Hamilton WL, Fairhurst RM, Tarning J, Winterberg M, Kwiatkowski DP,
497 Pukrittayakamee S, Hien TT, Day NP, Miotto O, White NJ, Dondorp AM. 2019. Determinants of
498 dihydroartemisinin-piperaquine treatment failure in Plasmodium falciparum malaria in Cambodia,
499 Thailand, and Vietnam: a prospective clinical, pharmacological, and genetic study. Lancet Infect
500 Dis 19:952–961.
501 32. Dhingra SK, Small-Saunders JL, Ménard D, Fidock DA. 2019. Plasmodium falciparum resistance to
502 piperaquine driven by PfCRT. The Lancet Infectious Diseases 19:1168–1169.
503 33. Kim J, Tan YZ, Wicht KJ, Erramilli SK, Dhingra SK, Okombo J, Vendome J, Hagenah LM,
504 Giacometti SI, Warren AL, Nosol K, Roepe PD, Potter CS, Carragher B, Kossiakoff AA, Quick M,
505 Fidock DA, Mancia F. 2019. Structure and drug resistance of the Plasmodium falciparum
506 transporter PfCRT. Nature 576:315–320.
507 34. Pelleau S, Moss EL, Dhingra SK, Volney B, Casteras J, Gabryszewski SJ, Volkman SK, Wirth DF,
508 Legrand E, Fidock DA, Neafsey DE, Musset L. 2015. Adaptive evolution of malaria parasites in
509 French Guiana: Reversal of chloroquine resistance by acquisition of a mutation in *pfcrt*. Proc Natl
510 Acad Sci USA 112:11672–11677.
511 35. Mairet-Khedim M, Leang R, Marmai C, Khim N, Kim S, Ke S, Kauy C, Kloeung N, Eam R, Chy S,
512 Izac B, Mey Bouth D, Dorina Bustos M, Ringwald P, Ariey F, Witkowski B. 2021. Clinical and In

513 Vitro Resistance of Plasmodium falciparum to Artesunate-Amodiaquine in Cambodia. Clin Infect
514 Dis 73:406–413.
515 36. Brenneman KV, Li X, Kumar S, Delgado E, Checkley LA, Shoue DA, Reyes A, Abatiyow BA,
516 Haile MT, Tripura R, Peto T, Lek D, Button-Simons KA, Kappe SHI, Dhorda M, Nosten F,
517 Nkhoma SC, Cheeseman IH, Vaughan AM, Ferdig MT, Anderson TJC. 2022. Optimizing bulk
518 segregant analysis of drug resistance using Plasmodium falciparum genetic crosses conducted in
519 humanized mice. iScience 25:104095.
520 37. Button-Simons KA, Kumar S, Carmago N, Haile MT, Jett C, Checkley LA, Kennedy SY, Pinapati
521 RS, Shoue DA, McDew-White M, Li X, Nosten FH, Kappe SH, Anderson TJC, Romero-Severson
522 J, Ferdig MT, Emrich SJ, Vaughan AM, Cheeseman IH. 2021. The power and promise of genetic
523 mapping from Plasmodium falciparum crosses utilizing human liver-chimeric mice. Commun Biol
524 4:734.
525 38. Willems A, Kalaw A, Ecer A, Kotwal A, Roepe LD, Roepe PD. 2023. Structures of Plasmodium
526 falciparum Chloroquine Resistance Transporter (PfCRT) Isoforms and Their Interactions with
527 Chloroquine. Biochemistry 62:1093–1110.
528 39. Osman ME, Mockenhaupt FP, Bienzle U, Elbashir MI, Giha HA. 2007. Field-based evidence for
529 linkage of mutations associated with chloroquine (pfcrt/pfmdr1) and sulfadoxine–pyrimethamine
530 (pfdhfr/pfdhps) resistance and for the fitness cost of multiple mutations in P. falciparum. Infection,
531 Genetics and Evolution 7:52–59.
532 40. Nair S, Li X, Arya GA, McDew-White M, Ferrari M, Nosten F, Anderson TJC. 2018. Fitness Costs
533 and the Rapid Spread of kelch13-C580Y Substitutions Conferring Artemisinin Resistance.
534 Antimicrob Agents Chemother 62:e00605-18.
535 41. Neumann C, Kulik L. 2014. Package"EloRating" (0.43).
536 42. Lekostaj JK, Natarajan JK, Paguio MF, Wolf C, Roepe PD. 2008. Photoaffinity labeling of the
537 Plasmodium falciparum chloroquine resistance transporter with a novel perfluorophenylazido
538 chloroquine. Biochemistry 47:10394–10406.
539 43. Wasakul V, Disratthakit A, Mayxay M, Chindavongsa K, Sengsavath V, Thuy-Nhien N, Pearson
540 RD, Phalivong S, Xayvanghang S, Maude RJ, Gonçalves S, Day NP, Newton PN, Ashley EA,
541 Kwiatkowski DP, Dondorp AM, Miotto O. 2022. Malaria outbreak in Laos driven by a selective
542 sweep for Plasmodium falciparum kelch13 R539T mutants: a genetic epidemiology analysis. Lancet
543 Infect Dis S1473-3099(22)00697–1.
544 44. Sudhakar R, Das D, Thanumalayan S, Gorde S, Sijwali PS. 2021. Plasmodium falciparum Atg18
545 localizes to the food vacuole via interaction with the multi-drug resistance protein 1 and
546 phosphatidylinositol 3-phosphate. Biochem J 478:1705–1732.
547 45. Wang Z, Cabrera M, Yang J, Yuan L, Gupta B, Liang X, Kemirembe K, Shrestha S, Brashear A, Li
548 X, Porcella SF, Miao J, Yang Z, Su X-Z, Cui L. 2016. Genome-wide association analysis identifies
549 genetic loci associated with resistance to multiple antimalarials in Plasmodium falciparum from
550 China-Myanmar border. Sci Rep 6:33891.
551 46. Breglio KF, Amato R, Eastman R, Lim P, Sa JM, Guha R, Ganesan S, Dorward DW, Klumpp-
552 Thomas C, McKnight C, Fairhurst RM, Roberts D, Thomas C, Simon AK. 2018. A single
553 nucleotide polymorphism in the Plasmodium falciparum atg18 gene associates with artemisinin
554 resistance and confers enhanced parasite survival under nutrient deprivation. Malar J 17:391.
555 47. Dhingra SK, Redhi D, Combrinck JM, Yeo T, Okombo J, Henrich PP, Cowell AN, Gupta P,
556 Stegman ML, Hoke JM, Cooper RA, Winzeler E, Mok S, Egan TJ, Fidock DA. 2017. A Variant
557 PfCRT Isoform Can Contribute to *Plasmodium falciparum* Resistance to the First-Line Partner
558 Drug Piperaquine. mBio 8:e00303-17.
559 48. Jumper J, Evans R, Pritzel A, Green T, Figurnov M, Ronneberger O, Tunyasuvunakool K, Bates R,
560 Žídek A, Potapenko A, Bridgland A, Meyer C, Kohl SAA, Ballard AJ, Cowie A, Romera-Paredes
561 B, Nikolov S, Jain R, Adler J, Back T, Petersen S, Reiman D, Clancy E, Zielinski M, Steinegger M,
562 Pacholska M, Berghammer T, Bodenstein S, Silver D, Vinyals O, Senior AW, Kavukcuoglu K,

563 Kohli P, Hassabis D. 2021. Highly accurate protein structure prediction with AlphaFold. Nature
564 596:583–589.
565 49. Varadi M, Anyango S, Deshpande M, Nair S, Natassia C, Yordanova G, Yuan D, Stroe O, Wood G,
566 Laydon A, Žídek A, Green T, Tunyasuvunakool K, Petersen S, Jumper J, Clancy E, Green R, Vora
567 A, Lutfi M, Figurnov M, Cowie A, Hobbs N, Kohli P, Kleywegt G, Birney E, Hassabis D, Velankar
568 S. 2022. AlphaFold Protein Structure Database: massively expanding the structural coverage of
569 protein-sequence space with high-accuracy models. Nucleic Acids Res 50:D439–D444.
570 50. Davis SZ, Singh PP, Vendrely KM, Shoue DA, Checkley LA, McDew-White M, Button-Simons
571 KA, Cassady Z, Sievert MAC, Foster GJ, Nosten FH, Anderson TJC, Ferdig MT. 2020. The
572 extended recovery ring-stage survival assay provides a superior association with patient clearance
573 half-life and increases throughput. Malar J 19:54.
574 51. Tirrell AR, Vendrely KM, Checkley LA, Davis SZ, McDew-White M, Cheeseman IH, Vaughan
575 AM, Nosten FH, Anderson TJC, Ferdig MT. 2019. Pairwise growth competitions identify relative
576 fitness relationships among artemisinin resistant Plasmodium falciparum field isolates. Malaria
577 Journal 18.
578 52. Amambua-Ngwa A, Button-Simons KA, Li X, Kumar S, Brenneman KV, Ferrari M, Checkley LA,
579 Haile MT, Shoue DA, McDew-White M, Tindall SM, Reyes A, Delgado E, Dalhoff H, Larbalestier
580 JK, Amato R, Pearson RD, Taylor AB, Nosten FH, D'Alessandro U, Kwiatkowski D, Cheeseman
581 IH, Kappe SHI, Avery SV, Conway DJ, Vaughan AM, Ferdig MT, Anderson TJC. 2023.
582 Chloroquine resistance evolution in Plasmodium falciparum is mediated by the putative amino acid
583 transporter AAT1. Nat Microbiol https://doi.org/10.1038/s41564-023-01377-z.
584 53. Neumann C, Duboscq J, Dubuc C, Ginting A, Irwan AM, Agil M, Widdig A, Engelhardt A. 2011.
585 Assessing dominance hierarchies: validation and advantages of progressive evaluation with Elo-
586 rating. Animal Behaviour 82:911–921.
587 54. Sen Ś, Churchill GA. 2001. A statistical framework for quantitative trait mapping. Genetics
588 159:371–387.
589 55. Broman KW, Wu H, Sen S, Churchill GA. 2003. R/qtl: QTL mapping in experimental crosses.
590 Bioinformatics 19:889–890.
591 56. Churchill GA, Doerge RW. 1994. Empirical threshold values for quantitative trait mapping.
592 Genetics 138:963–971.
593 57. Paradis E. 2010. pegas: an R package for population genetics with an integrated–modular approach.
594 Bioinformatics 26:419–420.
595

A.

Parasite name	KH004	Mal31
Origin	2016, Western Cambodia	2016, Malawi
Kelch13	C580Y	Wild-type
PfCRT	M74I, N75E, K76T, A220S, Q271E, N326S, I356T, R371I, **G367C**	Wild-type
Plasmepsin II/III Copy #	~4 copies	1 copy
PfAAT1	S258L, F313S	S258L
PfMDR1	Y184F	Y184F
PfMDR2	T484I, F423Y, G229D, S208N	I492V, S208N
Competitive fitness	Mild	Unfit

B.

PfCRT/PM Copy #/Plasmepsin	# of Available Progeny
M1M	47
M1K	10
M2K	13
M3K	7
M4K	3
M5K	4
K1M	8
K1K	3
K2K	7
K3K	1

Figure 1. Description of cross parents and progeny demographics. *A) KH004 is a multidrug Cambodian oarasite of the KEL1/PLA1 lineage and was isolated in 2016. It contains several traditional markers of drug resistance such as C580Y in Kelch13, a Dd2-like PfCRT with an additional G367C substitution, and multiple copies of plasmepsin II/III. Mal31 is a Malawi drug-sensitive parasite which has a wild-type genetic background at major resistance markers and expresses a single copy of plasmepsin II/III. B) Through our genetic cross, we have recovered 101 unique recombinant progeny which have various allelic combinations at pfcrt and pm. Progeny were grouped into 10 categories based on the allele inheritance at pfcrt and pm as well as pm copy number. K = allele inherited from KH004. M = allele inherited from Mal31*

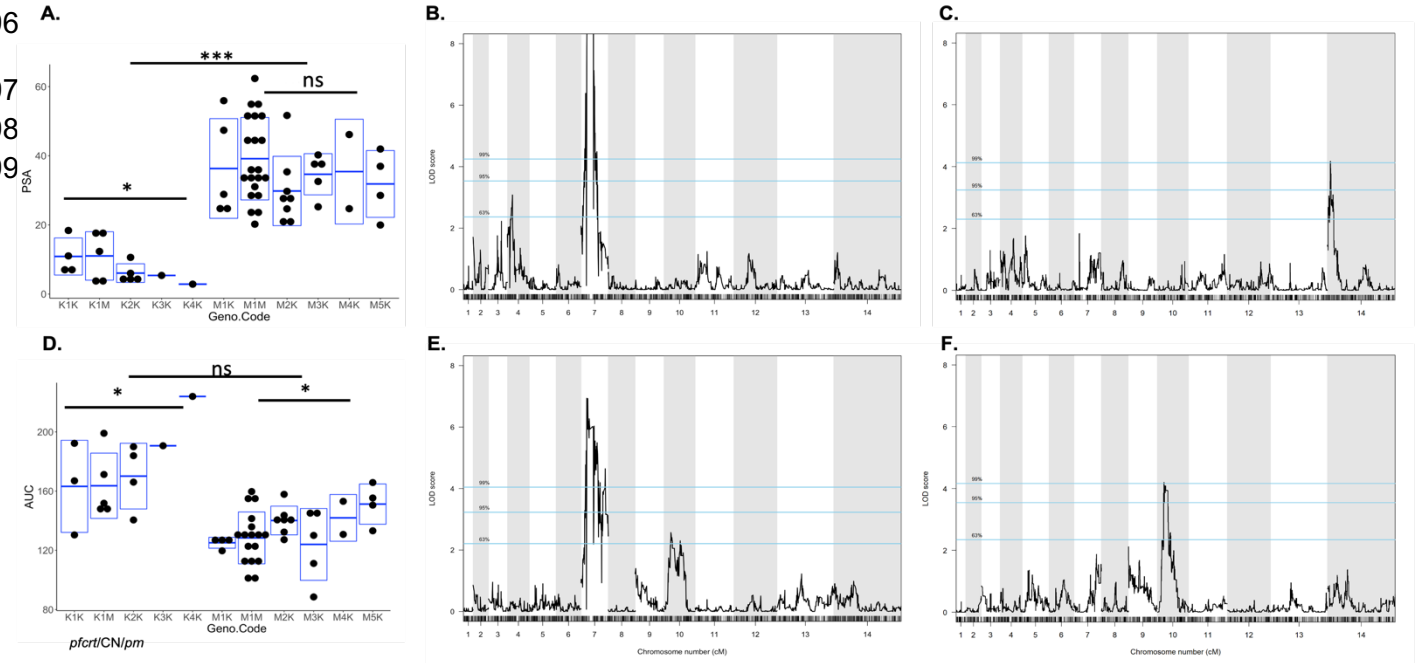

Figure 2: PfCRT is the major driver of PPQ-R. *A) Measuring PPQ sensitivity through PSA shows that inheritance of pfcrt allele is the major factor differentiating PPQ-R vs PPQ-S parasites. Additionally, pm copy number amplification further promotes resistance in a PPQ-R parasite expressing the KH004 pfcrt allele. PSA phenotype is represented in fold change between parasites exposed to 200nM PPQ and the no drug control. B) QTL mapping further supports the strong influence of pfcrt (chr 7 peak, LOD = 10.615) on PSA phenotype. C) Removal of the influence of pfcrt on this phenotype identifies a secondary region on chr 14, which encompasses plasmepsin II, influencing PPQ sensitivity through PSA. D) Measuring AUC phenotype reveals additive contributions of pm in parasites with either KH004 or Mal31 pfcrt alleles. E) Similar to QTL from PSA, we identify pfcrt as the major factor contributing to AUC phenotype, and residual scans F) identify a region within chr 10 that is associate with the AUC phenotype. This peak is centered around the gene atg18, which has previously been connected to PPQ-R. By using different phenotypes, we are still able to see the major role of pfcrt in PPQ-R parasites while also using these different phenotypes to identify novel secondary alleles associated with each phenotype.*

600

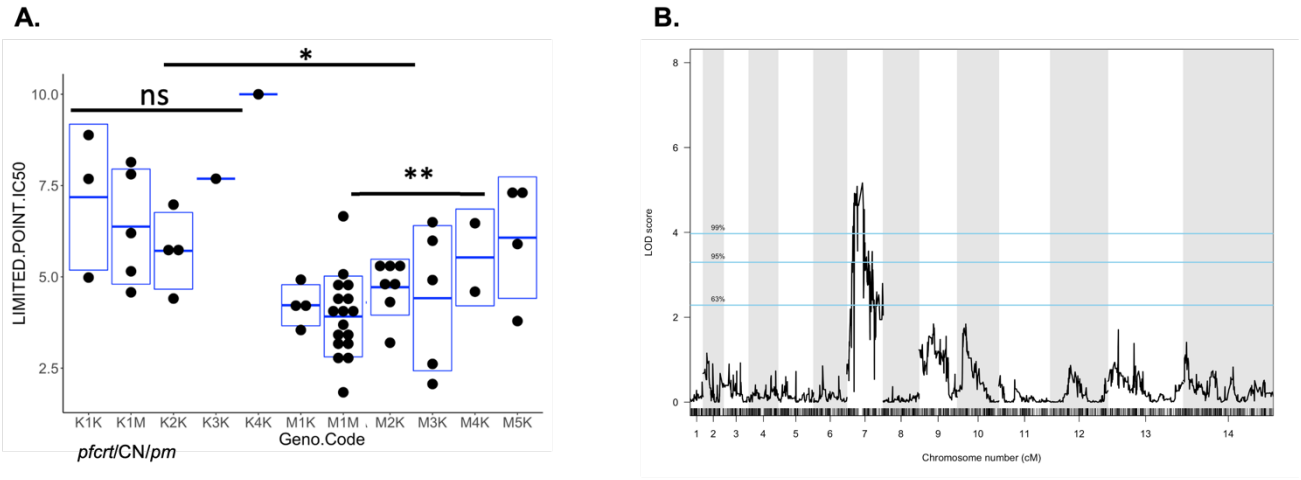

Figure 3: Additive role of *pm* copy number within PPQ-S population identified through LP-IC50. Using a limited point dose response curve allows us to calculate an IC50 independent of the biphasic nature of the curve. A) By using this modified IC50 phenotype, we see a significant difference in IC50 between *pfcrt* alleles as well as a decreased sensitivity associated with increased *pm* CN in a Mal31-*pfcrt* background. B) QTL mapping based on LP-IC50 solely associates *pfcrt* with this phenotype.

Country	% of PPQ-R samples	# of G367C samples	Nucleotide diversity (π)	Tajima's D
Cambodia (n = 1040)	37.5%	13	0.002600824	-0.8810487
Vietnam (n= 1325)	40.2%	14[a]	0.0033925	-0.8555029
Laos (n= 1061)	17.4%	3	0.005063148	-2.717986 **
Global population (n = 16203)		24		

Figure 4. Prevalence of G367C mutation in SEA. Based on available data from MalariaGen Pf7, this novel polymorphism has been observed throughout SEA, although at low levels, since 2012. Apart from two samples, this mutation is found in PPQ-R samples and is also accompanied by increased copies of *plasmepsin II/III*. Measurements of neutrality (Tajima's D) have identified an abundance of rare alleles which significantly deviates from mutation-drift equilibrium.

[a] Determination of resistance was based on *plasmepsin II/III* copy number amplification. Two samples from Vietnam carried a *single plasmepsin copy* and was deemed sensitive independent of *pfcrt* polymorphisms.

* $p < 0.05$ ** $p < 0.01$

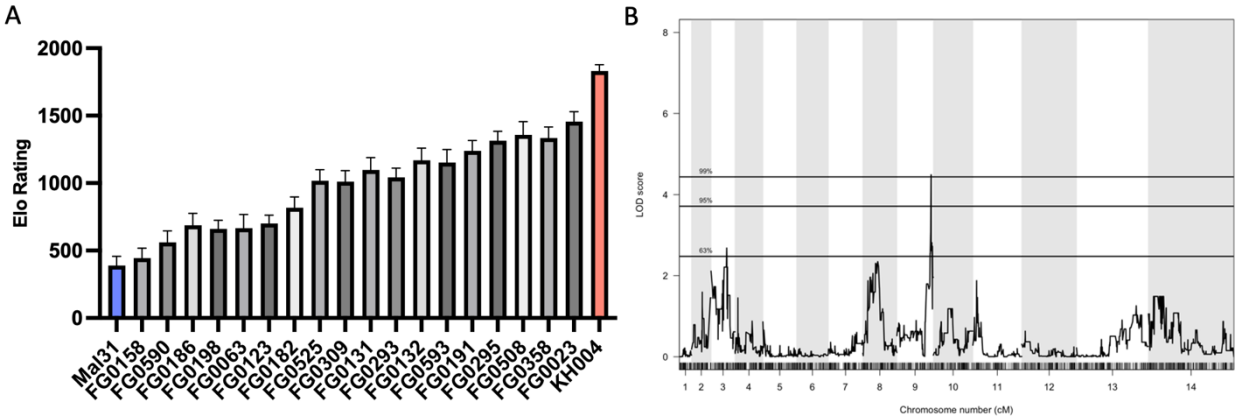

Figure 5. QTL mapping of fitness-associated loci using Elo rating phenotype. A) *Mean Elo rating of 18 progeny + 2 parents of the KH004 × Mal31 genetic cross based on 50 permutations of the order of competitions. Elo rating was calculated using the R package EloRating and was based on the each parasite's competitive growth assay outcome. Phenotype distribution is ordered from lowest Elo (least fit) on the left to highest Elo (most fit) on the right.* ***B)*** *QTL scan based on Elo phenotype reveals a highly significant peak (1% threshold) on chromosome 9. This peak encompasses a 35,264bp region which contains 15 genes. Genes identified from this QTL scan are proposed to directly contribute to parasite fitness.*

601
602

603 **Methods**

604

605 ***Parasites used in this study***

606 This study utilizes parents and progeny of the KH004 × Mal31 genetic cross generated by
607 utilizing human liver-chimeric mice and has previously been described in Brenneman et al (36).
608 From this cross, one hundred and one unique recombinant progeny were recovered through
609 limited dilution cloning at 0.3 cells per well. Individual wells containing parasites were identified
610 through qPCR and analysis of progeny relatedness and allele inheritance were based on the
611 methods outlined in Button-Simons et al. (37). Methods for sequencing of progeny, construction
612 of the genetic map, and generation of visual recombination map are all based on Button-Simons
613 et al. (37). Analysis of allelic co-inheritance utilized the entire progeny set of one hundred and
614 one parasites and phenotyping assays utilized fifty unique parasites, forty eight progeny and the
615 two parental parasites.

616

617 ***Parasite culture***

618 Cryopreserved *P. falciparum* stocks of KH004 × Mal31 progeny and KH004-020-019-H9
619 and Mal31-9040-C11 parents were thawed and cultured in complete media (CM) consisting of
620 0.5% Albumax II (Gibco, Life Technologies) supplemented RPMI 1640 with L-glutimate (Gibco,
621 Life Technologies) with additional 50 mg/L hypoxanthine (Calbiochem, Sigma-Aldrich), 25 mM
622 HEPES (Corning, VWR), 10ug/ml gentamycin (Gibco, Life Technologies), and 0.225% sodium
623 bicarbonate (Corning, VWR). Parasite cultures were maintained at 5% hematocrit in O+ red
624 blood cells (RBC) (Interstate Blood Bank, Memphis, TN) in separate flasks and maintained
625 consistent temperature (37ºC) and atmosphere (5% CO_2/5% O_2/90% N_2). Parasitemia of
626 cultures was kept below 2% and media changes were performed every 48 hours, corresponding
627 with one intraerythrocytic development cycle.

628

629 ***PfCRT Structure Analysis***

630 Three-dimensional homology model of PfCRT was predicted using AlphaFold (48, 49)
631 and accessed through the PDB database (6UKJ) (33). Additionally, the F′(ab) fragment used in
632 7G8 PfCRT cryo-EM structure elucidation (33) was removed from the structure. Protein
633 mutagenesis and visualization of resistance-associated mutations were conducted using PyMol
634 software (v2.5.4; Schrödinger, LLC).

635

636 ***Drug susceptibility assays***

637 Prior to susceptibility assay setup, parasites were synchronized using a single layer of
638 70% Percoll (Sigma Aldrich) in 1X RPMI with 13.3% sorbitol in phosphate buffered saline.
639 400µL of packed erythrocytes infected by a majority of schizont stage parasites were
640 resuspended in 2mL of incomplete media, layered over the percoll layer, and centrifuged (1561
641 x g for 10 in, no brake). The top layer was removed to isolate late-stage schizonts, washed
642 twice with incomplete media, resuspended at 5% hematocrit in complete media, and placed on
643 a shaker for 4 hours at 37ºC. Following the 4 hour incubation, parasitemia and stage were
644 determined through flow cytometry by staining with SYBR Green I and SYTO 61 and analyzed
645 on a Guava easyCyte HT (Luminex) after 50,000 events were counted. If cultures were >70%
646 ring-stage, they were diluted to 0.15% parasitemia at 2% hematocrit and set up in a 96-well
647 plate at a volume of 150µL per well. Within each assay plate, two technical replicates of each
648 parasite were exposed to 10 concentrations of a 2-fold dilution series of PPQ as well as both
649 untreated parasite and uninfected RBC controls. Parasites were exposed to PPQ for 72 hours.
650 Parasite density was determined using SYBR Green and dose-response curves were generated
651 by plotting percent survival against the log of drug concentration. Analysis of IC50 and AUC was
652 performed using Prism 9.0 (GraphPad). A nonlinear log inhibitor vs response 4 parameter dose-
653 response curve was generated based on percent survival. To generate the limited point curve,

654 data points which made up the biphasic portion of the plot were excluded to allow for a
655 sigmoidal shaped curve, which was then used for IC50 calculations.
656
657 ***PSA***
658
659 PSA was set up as originally described (18) with synchronized early ring stage parasites
660 being expose to a single 200nM dose of PPQ for 48 hours. This protocol was modified to
661 resemble the extended recovery RSA (eRRSA) phenotype (50), in which samples are analyzed
662 at 120 hours post-exposure instead of 72 hours. This extended timepoint has been shown to
663 provide superior differentiation between resistant and sensitive parasites and allows for finer
664 resolution between PPQ-S parasites. Parasite prevalence was measured through qPCR and
665 survival was calculated as fold change between untreated and treated samples for three
666 technical replicates (3 replicates within the plate as well as 3 independent qPCR reads) and at
667 least 3 biological replicates per sample. Additionally, to ensure consistency between our
668 resistance phenotypes, parasites from the same synchronization were used for both PSA and
669 IC50/AUC susceptibility assays.
670
671 ***Competitive growth assays***
672 To determine relative fitness levels between parasites, we used competitive growth
673 assays between progeny of the KH004 × Mal31 cross and both parental parasites as a proxy for
674 *in vitro* fitness. Parasitemia and stage of parasites was quantified using flow cytometry 15 hours
675 after synchronization with a 70% Percoll gradient. Synchronized parasites were each adjusted
676 to 0.5% parasitemia at 5% hematocrit and set up in a 1:1 ratio (1% total parasitemia) in 96-well
677 plates as previously described in (51, 52). Parasitemia was assessed (Giemsa-stained slides
678 and microscopy) every two days, in accordance with one intraerythrocytic life cycle, adjusted to
679 1% parasitemia and supplemented with fresh blood and media. Samples from each well were
680 collected at regular intervals upon sample dilution and stored at -80ºC for genotyping. These

681 competitive growth assays were maintained for a maximum of 40 days, or until one parasite
682 reached fixation (>95% of the co-culture). Parasites were deemed to have equivalent fitness
683 levels if by 40 days neither parasite reached fixation.
684
685 To analyze relative parasite densities in each competition, six microsatellite markers
686 (MS) were used for genotyping (Supplementary Table 4) to differentiate parasites in co-culture.
687 PCR amplification was performed using the Phusion Blood Direct PCR Kit (ThermoFisher, cat
688 #F547L) for 30 cycles as previously described in (51). Amplified microsatellites were analyzed
689 using the Applied Biosystems 3730xl DNA Analyzer (ThermoFisher). Raw fragment analysis
690 data was uploaded to the Thermo Fisher Connect platform and analyzed using the microsatellite
691 analysis tool. The proportion of the two competing parasites in co-culture was determined by
692 taking the ratio of fluorescent peak height associated with the corresponding PCR product size.
693
694 Due to the large number of competitive growth assays required to directly compete all
695 parasites against each other, all parasites were competed against both parents. Additionally, a
696 genetically diverse subset of parasites were competed against each other. Based on the
697 outcomes of the progeny v progeny competitions, an Elo rating system, which has previously
698 been used for animal dominance hierarchies, was utilized to assign a quantitative score to each
699 parasite based on their win/loss record while also taking into account the record of the parasite
700 competed against (53). The package “EloRating” (41) in R Studio (2023.03.0+386). was used
701 for assigning scores. In order to reduce the effect of competition order on ranking, the
702 competitive outcomes file was randomized 1000 times to generate 1000 Elo scores which were
703 then averaged. The distribution of Elo ratings figure was created using Prism 9.0 (GraphPad).
704
705
706

707 ***QTL Analysis***

708 Statistical analysis of the QTL data for this cross was performed using the computational
709 methods previously described (54). Blood stages of *P. falciparum* are haploid, therefore, only
710 two genetic classes are present for each locus. QTL mapping was performed using the "R/qtl"
711 package (55) in R Studio. One thousand permutations of the trait values determined the 37%,
712 5%, and 1% genome-wide significance thresholds and the strength of each linkage was
713 expressed as a logarithm of the odds (LOD) score (56). The main QTL and corresponding mean
714 trait values from these scans were used to obtain estimates of residual empirical thresholds to
715 identify secondary loci that contribute to the phenotype of interest (56)

716

717 ***Global haplotype analysis***

718 Analysis of global *pfcrt* haplotypes was performed using publicly available sequences
719 through the Pf7 dataset (MalariaGen) (12). PPQ resistance status for this dataset was inferred
720 based on *plasmepsin II/III* amplification, therefore, all samples labeled as PPQ-R are assumed
721 to express more than one copy of these genes. Tajima's D and nucleotide diversity were used
722 as metrics of genetic diversity within and were calculated using the R package "pegas" (57).

723
724
725
726
727

Additional Information

Additional figures and tables are available for this paper.

Correspondence and requests for materials should be addressed to Michael T. Ferdig (ferdig.1@nd.edu)

Funding

National Institutes of Health grant P01 12072248 (MTF)